

## Self-assembled molecular films of tetraamino metal (Co, Cu, Fe) phthalocyanines on gold and silver. Electrochemical and spectroscopic characterization\*

M. P. Somashekarappa<sup>1</sup>, J. Keshavayya<sup>2</sup>, and S. Sampath<sup>1,‡</sup>

<sup>1</sup>Department of Inorganic and Physical Chemistry, Indian Institute of Science, Bangalore 560 012, India; <sup>2</sup>Department of Industrial Chemistry, Kuvempu University, Shimoga Karnataka, India

**Abstract:** The formation of molecular films of 2,9,16,23-tetraamino metal phthalocyanines [TAM(II)Pc; M (II) = Co, Cu, and TAM(III)Pc; M = Fe] by spontaneous adsorption on gold and silver surfaces is described. The properties of these films have been investigated by cyclic voltammetry, impedance, and FT-Raman spectroscopy. The charge associated with Co(II) and Co(I) redox couple in voltammetric data leads to a coverage of  $(0.35 \pm 0.05) \times 10^{-10}$  mol cm<sup>-2</sup>, suggesting that the tetraamino cobalt phthalocyanine is adsorbed as a monolayer with an almost complete coverage. The blocking behavior of the films toward oxygen and Fe(CN)<sub>6</sub><sup>3-/4-</sup> redox couple have been followed by cyclic voltammetry and impedance measurements. This leads to an estimate of the coverage of about 85 % in the case of copper and the iron analogs. FT-Raman studies show characteristic bands around 236 cm<sup>-1</sup> revealing the interaction between the metal substrate and the nitrogen of the -NH<sub>2</sub> group on the phthalocyanine molecules.

### INTRODUCTION

Phthalocyanines have been shown to have very interesting properties coupled with excellent stability to heat, light, and harsh chemical environments. Their optical and electronic properties have been exploited in various applications such as pigments in paints and printing inks; infrared security devices, information storage, and computer disk writing; conducting polymers and photoconductors; catalysts for oxidation of thiols, disulfides, chemical sensors, and in photodynamic therapy of cancer [1,2]. Transition metal-based phthalocyanines have attracted attention in the areas of fuel cells, gas sensors, and biosensors [1,2]. Most of these applications require the use of phthalocyanines in the form of thin films. Further, it is desirable to have ordered, well-packed, and oriented molecular layers of phthalocyanines on various substrates.

Chemisorption of molecules onto metal substrates offer the flexibility of molecular ordering and orientation. In this direction, self-assembled films of thiols, disulfides, silanes, and nitrogen containing compounds onto gold, silver, and platinum substrates have been receiving wide attention [3–6]. The potential use of these molecular films for the study of electron-transfer kinetics, wetting, corrosion, tribology, sensing, and other applications have already been demonstrated [3,7–10].

\*Pure Appl. Chem. 74, 1489–1783 (2002). An issue of reviews and research papers based on lectures presented at the 2<sup>nd</sup> IUPAC Workshop on Advanced Materials (WAM II), Bangalore, India, 13–16 February 2002, on the theme of nanostructured advanced materials.

‡Corresponding author: E-mail: sampath@ipc.iisc.ernet.in

The study of adsorbed molecular films of phthalocyanines includes the following: Cook, Russell, and coworkers have reported the preparation of phthalocyanines with one or two trichlorosilyl alkyl chains and subsequently formed self-adsorbed films on glass and silicon [11]. The preparation and film formation of the thiol and disulfide-derivatized phthalocyanines [12–14] on gold surfaces have been accomplished by the same group. The infrared reflection–absorption spectroscopy (IRRAS) and evanescent wave-excited fluorescence emission studies have been used to identify the orientation of the phthalocyanine monolayers. These studies suggest that the orientation of the phthalocyanine ring of the molecule depends on the length of the spacer between the ring and the gold surface. When the chain length is large and is of the order of C11 hydrocarbon chain, the macrocycles assume a densely packed orientation with the phthalocyanine ring arranged perpendicular to the gold surface. A C3 alkyl chain induces the formation of a less closely packed monolayer with the phthalocyanine rings arranged parallel to the gold surface. Huc and coworkers [15] reported that ruthenium phthalocyanine can be grafted onto gold substrates by axial ligation using isonitriles as spacers between the metal and the phthalocyanine. Recently, Li and coworkers have reported the formation of self-assembled monolayers (SAMs) of thiol-tethered, octasubstituted, and axially ligated silicon phthalocyanines [16]. However, a careful examination of the literature reveals that the formation of spontaneously adsorbed metal phthalocyanine molecular films on metal substrates, and their applications have not been explored in detail. The metal phthalocyanines constitute an important class of compounds that provide models for theoretical and experimental studies involving electron-mediated processes [17]. One of the main areas of interest is the electrocatalytic reduction of oxygen by metal phthalocyanines [18–19]. In this paper, we describe the molecular film formation of 2,9,16,23-tetraamino metal phthalocyanines [metal = Co(II), Cu(II), and Fe(III)] on gold and silver surfaces. Electrochemical methods and FT-Raman spectroscopy have been used to characterize these films.

## EXPERIMENTAL

### Preparation of the metal phthalocyanines

2,9,16,23-Tetraamino Co(II) phthalocyanine [TACo(II)Pc], 2,9,16,23-tetraamino Cu(II) phthalocyanine [TACu(II)Pc], and 2,9,16,23-tetraamino Fe(III) phthalocyanine [TAFE(III)Pc] were prepared and purified following the reported procedure [20–22].

4-Nitrophthalic acid and sodium sulfide nonahydrate were procured from Lancaster, UK. All other chemicals and solvents used were of analytical grade. Double-distilled water was used in all the preparations. The cobalt analog is prepared using the following procedure. Briefly, a finely ground mixture of 4-nitrophthalic acid (10.0 g, 0.09 mol),  $\text{CoSO}_4 \cdot 7\text{H}_2\text{O}$  (7.5 g, 0.03 mol), ammonium chloride (5.0 g, 0.09 mol), urea (30.0 g, 0.49 mol) and a catalytic amount of ammonium molybdate was stirred in a 500-mL round-bottomed flask containing nitrobenzene solvent (15 mL) at 180 °C for 5 h. The resulting crude product was ground and washed with methanol repeatedly until the solvent was completely removed. It was further stirred in 1 M HCl (500 mL) saturated with NaCl for 5 min and filtered. The residue was then washed using 1 M NaOH (500 mL) saturated with NaCl at 90 °C until the evolution of  $\text{NH}_3$  ceased. The resulting product was centrifuged and further treated with NaCl-saturated HCl and NaOH solutions a few times. The bluish-green product, 2,9,16,23-tetranitro cobalt (II) phthalocyanine was washed with water until free from chloride ions, centrifuged and dried in vacuum over  $\text{P}_2\text{O}_5$ . The reduction of the nitro groups was carried out by stirring 2,9,16,23-tetranitro cobalt (II) phthalocyanine (10.0 g, 0.01 mol) in an aqueous solution (250 mL) of sodium sulfide nonahydrate (50.0 g, 0.21 mol) at 50 °C for 5 h. The solid product was separated in a centrifuge and treated with 1 M HCl (500 mL). The residue was separated and treated with 1 M NaOH (500 mL), stirred for 1 h, and centrifuged to separate the solid complex. The product was repeatedly washed with water until free from NaOH and NaCl. The pure 2,9,16,23-tetraamino cobalt(II) phthalocyanine was dried in vacuum over  $\text{P}_2\text{O}_5$ . The product was characterized by elemental analysis for C, H, N, and Co, UV–vis and IR spec-

trospectroscopy and powder X-ray diffraction techniques, and the results were in conformity with those reported in the literature [20–22].

The copper and iron analogs of the aminophthalocyanines were prepared by using stoichiometric amounts of  $\text{CuSO}_4 \cdot 5\text{H}_2\text{O}$  or anhydrous  $\text{FeCl}_3$ , respectively, in place of  $\text{CoSO}_4 \cdot 7\text{H}_2\text{O}$  in the above procedure. These phthalocyanine analogs were also characterized using the same techniques as described above and were found to be in agreement with the reported results [20,22].

### Formation of adsorbed molecular films

The adsorbed phthalocyanine molecular films were formed on gold and silver disk electrodes of geometric area  $0.031 \text{ cm}^2$ . Gold electrodes were polished on a polishing cloth using  $0.05\text{-}\mu\text{m}$  alumina and washed thoroughly with water. They were subsequently cleaned by immersing in piranha solution (a mixture of sulfuric acid and hydrogen peroxide in the ratio 3:1 by volume) for 15 s. *Caution: piranha solution is very reactive with organic compounds, and direct contact should be avoided.* This procedure was repeated several times until reproducible cyclic voltammograms were obtained for the oxidation of  $\text{Fe}(\text{CN})_6^{4-}$  in KCl solutions. Silver electrodes were polished on a polishing cloth using  $0.05\text{-}\mu\text{m}$  alumina suspension and subsequently washed with double-distilled water followed by washing with absolute alcohol. This procedure was repeated several times until a reproducible cyclic voltammogram was obtained for the reduction of oxygen in a phosphate buffer of pH 7.

Molecular films of cobalt phthalocyanine were formed by immersing the clean electrodes in a saturated solution of phthalocyanine in *n*-butanol. *n*-Butanol was preferred due to the ease of evaporation of the solvent. Copper phthalocyanine films were formed using a similar procedure while the iron analog was assembled from a 3 mM aqueous solution for 24 h. Solubility criteria was used in choosing different solvents. The electrodes were removed and rinsed with the respective solvents for about 30 min, followed by thorough washing in ethanol and water. The modified electrodes were stored in the respective solvents and then used for characterization.

### Characterization

Bruker IFS 100/S FT-Raman spectrometer with Nd-YAG laser source with a wavelength of 1064 nm was used for the FT-Raman studies. The scattered signals were collected at an angle of  $180^\circ$  to the incident laser beam. The laser power used for the films on silver, gold, and glass was 300 and 100 mW for the solution studies. The films were found to be stable despite the high laser power used. Samples for FT-Raman measurements were prepared by adsorbing the phthalocyanines on electrochemically roughened gold and silver surfaces. The electrochemical pretreatment was carried out by repeated cycling of the electrodes between  $-0.155$  and  $1.245 \text{ V}$  in  $0.5 \text{ M H}_2\text{SO}_4$  in the case of gold [23] and between  $-0.65$  and  $0.15 \text{ V}$  in  $0.1 \text{ M KCl}$  in the case of silver [24]. The roughness of the electrodes was measured using a profilometer (Form Talysurf plus, UK) that scans a particular section on the surface, and a surface amplitude profile is given as the output. The average is taken to be the roughness of the surface. Five different regions were scanned on the surface, and all of them lead to a roughness of  $(60 \pm 2) \text{ nm}$  for gold and  $(30 \pm 3) \text{ nm}$  for silver. In electrochemistry literature, however, the roughness factor is given as the ratio of the true area to the geometric area of the electrode. This ratio is determined based on the charge associated with the reduction of gold oxide in a  $0.5 \text{ M H}_2\text{SO}_4$  solution [25] in the case of gold electrode and the capacitive currents associated with the cyclic voltammograms in  $0.1 \text{ M HClO}_4$  in the case of silver electrode [26]. The roughness factors were calculated to be 3.6 for gold and 6.8 for silver electrodes. The profilometer-based roughness is generally used in explaining the enhancement in Raman signals arising from the adsorbed molecules, while the electrochemically determined roughness factor is used to determine the true electrochemical parameters such as coverage, surface concentration, number of electrons involved in the redox process, etc.

The roughened surfaces were used for assembling the films as described above. After the formation of the films, the samples were washed very well with the same solvent for 30 min and subsequently washed with absolute alcohol. Further, the samples were dried over silica gel in the atmosphere of ultra-high purity argon for 1 h before the measurements. Raman spectra were also recorded on a thin film of the compound on a glass plate and in 1 mM solution in dimethylformamide (DMFO) for comparison.

Electrochemical measurements were carried out using either Versastat II (EG&G, Princeton, NJ) or a CHI 660A electrochemical analyzer (CH instruments, Austin, Texas). A three-electrode cell consisting of a saturated calomel reference electrode, a platinum foil counterelectrode, and the modified silver or gold disc as working electrode was used. The cell was purged with purified nitrogen or argon whenever required.

## RESULTS AND DISCUSSION

The structures of phthalocyanine molecules used in the present study are shown in Fig. 1. Cobalt(II) and copper(II) phthalocyanines are planar (Fig. 1a), while the iron(III) analog has axially chlorine-ligated square pyramidal structure (Fig. 1b) [27]. The formation of phthalocyanine molecular films on the metal surfaces is confirmed by checking the blocking behavior of the films for soluble, redox-active compounds. Figure 2a shows the cyclic voltammograms of bare and [TAFE(III)Pc]-modified gold electrodes in a phosphate buffer solution of pH 7. The bare metal surface shows a single, irreversible reduction

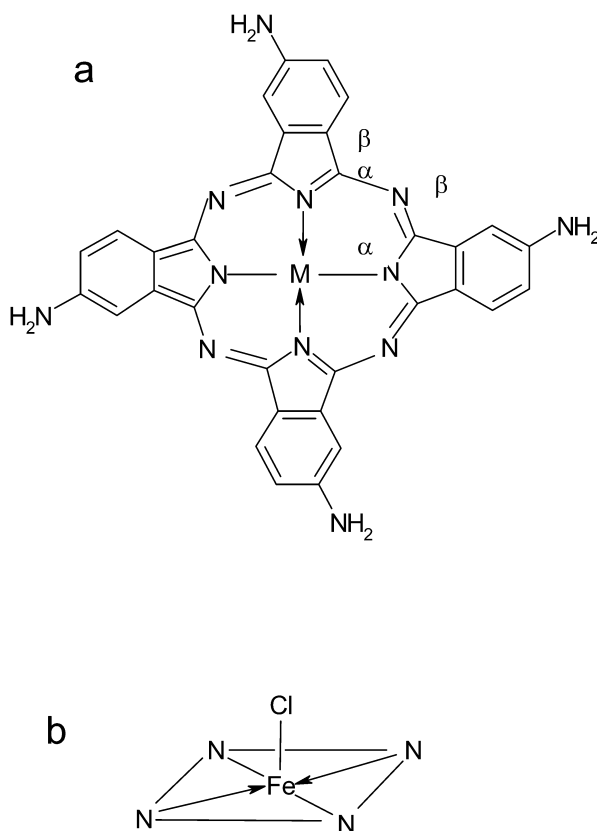


**Fig. 1** (a) Structure of 2,9,16,23-tetraamino metal phthalocyanine where, M = Co(II), Cu(II), and Fe(III). (b) Square pyramidal structure of axially chlorine-ligated metal core in iron phthalocyanine.

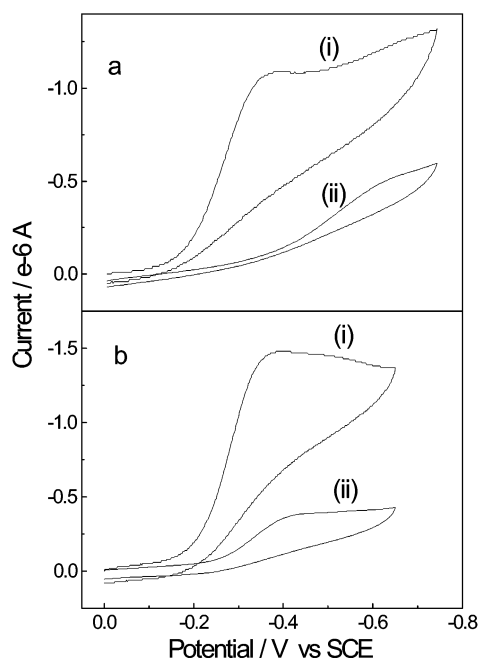


**Fig. 2** Cyclic voltammograms for oxygen reduction on (a) gold and (b) silver electrodes in 0.1 M phosphate buffer, pH 7 at 25 °C. (i) refers to the bare metal surface and (ii) refers to the TAFE(III)Pc covered surface. The scan rate used was 10 mV/s.

peak for dissolved oxygen at  $\sim -0.4$  V, while the covered electrode blocks the access of oxygen molecules leading to decreased currents at the same applied DC bias potentials. It is clear from the negative shift in the reduction peak potentials and the decrease in peak currents, that the films have blocking characteristics for soluble redox-active compounds. Based on the relative decrease in Faradaic currents at the peak potential, the coverages have been estimated to be  $(90 \pm 2)$  % on gold and  $(80 \pm 2)$  % on silver surfaces. The ability of the coated electrodes to block the electron transfer between the metal surface and a soluble redox mediator is a direct measure of the defectiveness associated with the blocking film [28–30]. A freely diffusing mediator will react exclusively at the pinholes/defects if the electron transfer is blocked across the majority of the monolayer. Hence, the ratio of the Faradaic currents observed at the formal potential of a redox mediator on a bare and a coated electrode could be an indirect measure of the defectiveness or the coverage. The blocking behavior of the modified electrode for another soluble redox species,  $\text{Fe}(\text{CN})_6^{4-}$ , has also been followed by impedance measurements (Fig. 3). The comparison of the total impedance in the impedance plots recorded on bare and the [TAFE(III)Pc] and [TACu(II)Pc] film-coated electrodes shows the effect of the adsorbed film. The plots (ii) in Fig. 3 illustrate the blocking behavior of the film with well-defined semicircles at higher frequencies. The diameter of this semicircle is a measure of the charge-transfer resistance ( $R_{\text{ct}}$ ). This  $R_{\text{ct}}$  on the covered electrode is greater than the  $R_{\text{ct}}$  measured for bare gold electrode owing to the inhibition to the charge-transfer rate [31]. The charge-transfer resistance ( $R_{\text{ct}}$ ) calculated for the bare gold surface is  $24.4 \Omega \text{ cm}^2$ , while the  $R_{\text{ct}}$  for the covered electrode works out to be  $154.0 \Omega \text{ cm}^2$ . The relative increase in  $R_{\text{ct}}$  values for a covered surface as compared to the bare surface reflects the poor accessibility of the probe species to the electrode. Based on these values, the coverage is calculated to be  $(84 \pm 3)$  %. Impedance measurements were not carried out on silver since the metal oxidation at these dc bias potentials [formal redox potential of  $\text{Fe}(\text{CN})_6^{3-/4-}$  is around 0.2 V] interferes with the measurements. Copper analog of the phthalocyanine shows a similar behavior, and the coverage on gold calculated based on cyclic

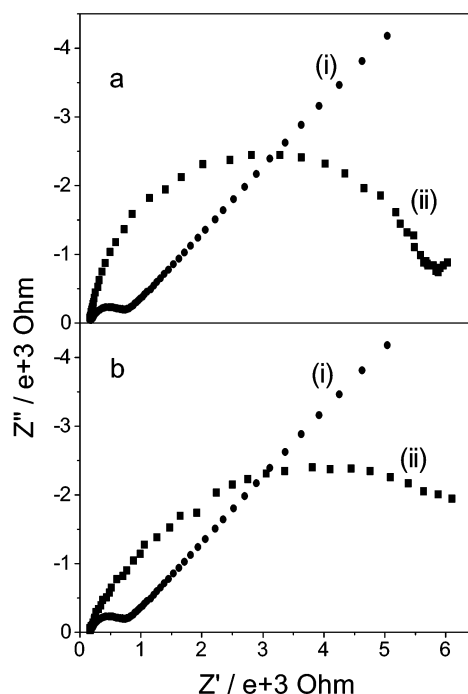


**Fig. 3** Impedance plots for gold covered with (a) TAFE(III)Pc and (b) TACu(II)Pc films in a 0.1 M KCl solution containing 1 mM  $K_3Fe(CN)_6$  and 1 mM  $K_4Fe(CN)_6$ . (i) refers to the bare surface and (ii) refers to the phthalocyanine-modified surface. The frequency range used is 0.1 to  $10^5$  Hz.

voltammetry is  $(84 \pm 2) \%$ , while it works out to be  $(83 \pm 3) \%$  based on impedance measurements using ferricyanide/ferrocyanide redox couple. The cobalt analog alone is found to catalyze the electrochemical processes, and, hence, the coverage studies are carried out using the surface electrochemistry as given below. The electrocatalytic reduction of oxygen is believed to be dependent on the orientation of the phthalocyanine molecules on the electrode surface, and this is being probed further.

### Surface electrochemistry of the phthalocyanine films

Cyclic voltammetric studies have been carried out in deaerated buffer solutions, to understand the electrochemical behavior of the phthalocyanine films. This provides an easy way to explore the redox properties of phthalocyanines in the absence of potentially complicating solution equilibria. The stability of the adsorbed cobalt phthalocyanine films under electrochemical conditions is far superior to the corresponding copper and iron analogs. Moreover, [TACo(II)Pc] films are found to electrocatalyze the reduction of oxygen. This aspect is addressed in a separate paper. Hence, a detailed investigation is carried out on the surface electrochemistry of cobalt phthalocyanine films. Electrochemical studies on cobalt phthalocyanine and various substituted cobalt phthalocyanines have been investigated by adsorbing them on glassy carbon and different kinds of graphite electrodes like highly oriented pyrolytic graphite (HOPG), basal plane pyrolytic graphite (BPG), etc. [19,32–36]. Figure 4a shows the cyclic voltammogram of TACo(II)Pc adsorbed onto silver electrodes, in a phosphate buffer of pH 7. The scans were carried out between 0.05 V and  $-0.9$  V vs. SCE. Two well-defined, redox peaks are observed with formal potentials at  $-0.24$  V and  $-0.66$  V, at a scan rate of 200 mV/s. The redox peaks labeled II are associated with [TACo(II)Pc( $-2$ )] / [TACo(I)Pc( $-2$ )]<sup>-</sup> couple. The formal potential value of this couple,  $E_f^0$ , agrees well with the literature reports on the Co(II)/Co(I) couple of the cobalt phthalocyanines [19,32,34,37],

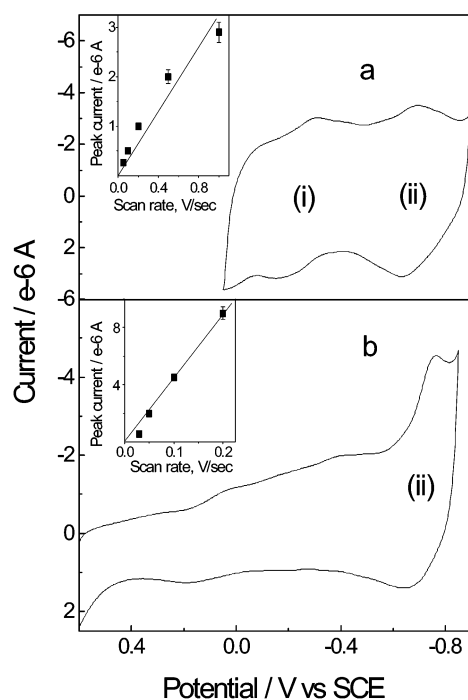


**Fig. 4** Cyclic voltammograms of TACo(II)Pc modified (a) silver and (b) gold electrodes in a pH 7, 0.1 M phosphate buffer solution. The scan rate used was 200 mV/s. (i) and (ii) are explained in the text. Inset: Plots of peak current versus scan rate for the anodic peak of the couple (II) in the respective cyclic voltammograms.

particularly the tetraaminated phthalocyanine [19]. Surface-confined species generally lead to very symmetric waves without any peak separation between the anodic and cathodic peak positions. The full width at half-maximum (fwhm) is expected to be 0.096 V for an ideal, reversible, one-electron reaction of an adsorbed species [38]. However, in the present study, a peak split of 0.15 V and 0.065 V are observed at a scan rate of 0.2 V/sec for peaks (i) and (ii), respectively (Fig. 4a). When the fwhm values are analyzed, it is apparent that these are higher than the expected 0.096 V. These observations point on the kinetic limitations or repulsive interactions of the molecules in the film. A plot of the peak current vs. scan rate [for both the anodic (inset, Fig. 4a) and cathodic processes] is found to be linear, as expected for a surface-confined species. These values are corrected for the large base currents observed. The cause of the large capacitive currents in the cyclic voltammograms is presently unknown, but we speculate that this may have its origin in the dielectric properties of the adsorbed films. The films are very stable, and the peak currents stay constant with repeated cycling in the potential range between 0.05 and  $-0.9$  V. This is contrary to the observations of Lever and coworkers [19] where a physisorbed film of the tetraamino phthalocyanine on an HOPG electrode was found to be unstable. The stability on HOPG surface was reported to increase when the phthalocyanine film was polymerized on the surface by cycling the potential to positive values. In the present case, the adsorbed monomolecular film itself is found to be very stable even after repeated cycles.

The assumption that the adsorbed phthalocyanine films lead to a one-electron redox process at  $-0.66$  V was checked as follows. The number of electrons,  $n$ , is related to the peak width at half-maximum (pwhm,  $W_{1/2}$ ) if a Langmuir-type adsorption isotherm is assumed as,  $n = 2RT\{\ln(3 + 2\sqrt{2})/FW_{1/2}\}$ . This results in a value of 0.7 for  $n$ . The departure from unity may be due to the interaction between adjacent molecules that would lead to a deviation from an exact Langmuir-type of adsorption isotherm. In self-assembled monolayer systems based on alkane thiols, interactions between adjacent molecules are

well known [3]. Moreover, the use of any isotherm requires a dynamic equilibrium between surface and bulk, and the absence of phthalocyanine molecules in the bulk phase precludes such an equilibrium in the present study. Considering the peak at  $-0.66$  V as a one-electron redox couple, a surface concentration of  $(0.35 \pm 0.05) \times 10^{-10}$  mol  $\text{cm}^{-2}$  has been calculated for the real surface area based on the roughness factor mentioned earlier. If the phthalocyanine molecules are lying flat on the surface, yielding an area of approximately  $200 \text{ \AA}^2$  [19,35], the coverage,  $\Gamma$ , should work out to be  $0.8 \times 10^{-10}$  mol  $\text{cm}^{-2}$ . Hence, the present coverage leads to approximately one monolayer [35,39]. However, the small difference may be due to the  $n$  value being different from one. Figure 4b shows the cyclic voltammogram of the adsorbed cobalt phthalocyanine on a gold surface. It is observed that the stability of the film is low. Repeated cycling leads to a continuous decrease in peak currents. Following the procedure of Lever [19], the as-prepared film was oxidized by cycling the electrode to more positive potentials. The resulting cyclic voltammogram (Fig. 4b) is very similar to the one observed for the polymerized amino phthalocyanine films on a HOPG electrode [19]. The redox waves observed at around  $-0.2$  V were also observed on HOPG [19], and this was tentatively assigned to the oxidation of the polyaniline-like components of the polymer film in addition to a contribution from the first-ring oxidation process [40]. However, we believe that the ring oxidation is more probable than the first possibility of the oxidation of polyaniline-like components. This is based on the fact that the redox wave at  $-0.2$  V is observed on a silver surface as well (Fig. 4a), wherein the phthalocyanine film is present in the monomer form (the potential of cycling is from  $0.05$  to  $-0.9$  V) and not polymerized. The relative stability variations on the gold and silver surfaces may be due to the affinity of the  $-\text{NH}_2$  groups being higher for silver than for gold electrodes.

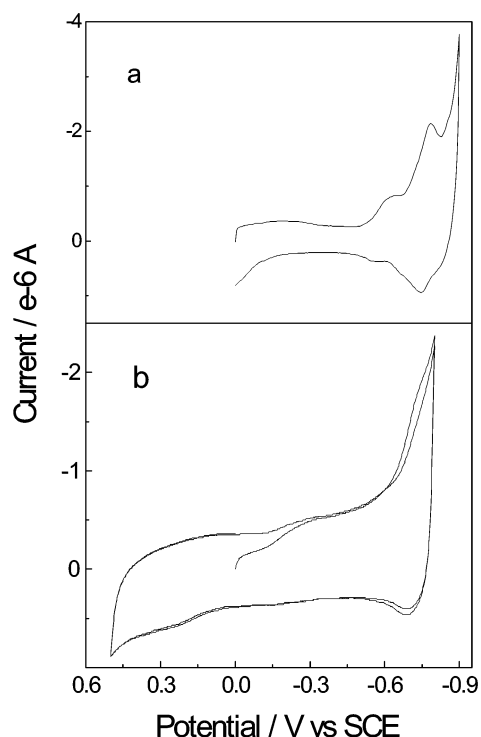


**Fig. 5** Cyclic voltammograms of TACu(II)Pc modified (a) silver and (b) gold electrodes in a pH 7, 0.1 M phosphate buffer solution. The scan rates used were 50 mV/s in the case of silver and 100 mV/s in the case of gold.



The surface electrochemistry of TACu(II)Pc films adsorbed on gold electrodes (Fig. 5b) yields a redox couple at around  $-0.7$  V. This is attributed to the ring reduction as,  $[\text{Cu}^{2+}, \text{Pc}^{2-}] + e \rightleftharpoons [\text{Cu}^{2+}, \text{Pc}^{3-}]^-$ . Further, redox waves observed at  $-0.3$  and  $+0.3$  V may be attributed to the  $[\text{Cu}^{2+}, \text{Pc}^{2-}] + e \rightleftharpoons [\text{Cu}^+, \text{Pc}^{2-}]^-$  reaction, as reported for the polymerized film of copper phthalocyanine on glassy carbon electrodes [41]. The TACu(II)Pc films on silver surfaces result in redox couples at  $-0.75$  and  $-0.6$  V, the one at  $-0.75$  V (Fig. 5a) may be attributed to the ring reduction process as in the case of gold. However, it should be pointed out that the stability of the copper phthalocyanines on gold as well as on silver surfaces is poor and repeated cycling results in the diminishing of peak currents.

The electrochemical stability of the adsorbed iron phthalocyanine films in aqueous medium on both the electrodes is lower than the copper and cobalt analogs. The film electrochemistry of the TAFE(III)Pc films in phosphate buffer solutions on silver electrodes shows the presence of three redox peaks at potentials close to  $-0.1$ ,  $-0.65$ , and  $-0.8$  V (figure not shown). The peaks at  $-0.1$  and  $-0.65$  may be assigned to the Fe(III)/Fe(II) and Fe(II)/Fe(I) couples based on the reported values in the literature for iron phthalocyanine [33]. The third couple is assigned to the ring reduction as given earlier.

### FT-Raman studies

FT-Raman spectroscopy with an excitation wavelength of 1064 nm using a Nd:YAG laser has the advantage of being a “fluorescence-free” Raman technique. Recent studies on near-infrared surface enhancement (FT-SERS) has shown enhancement factors of  $10^5$ – $10^6$  with various metal substrates such as Au, Ag, and Cu [42]. In the present studies, we have characterized the adsorbed phthalocyanine films on roughened metal surfaces, using FT-Raman scattering technique. The electrochemical characteristics of the films formed on polished as well as roughened metal surfaces are found to be similar. The films were washed very well to ensure that the weakly physisorbed phthalocyanine is completely removed. Despite the high complexity of the molecule, the Raman lines are clearly detectable. It is known that when the density of the molecules in the film is small and the interaction among them is negligible, the measured Raman intensity directly reflects the magnitude of the absolute scattering cross-section of individual molecules [43]. Metallophthalocyanines have a sufficiently large Raman cross-section, and it may be expected that a high signal-to-noise ratio will be obtained in the spectra [43,44].

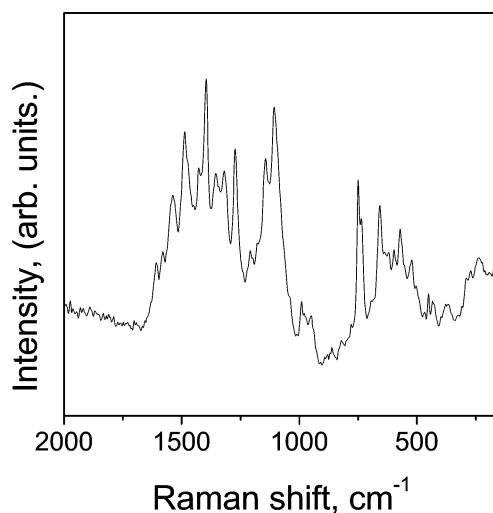


Fig. 6 FT-Raman spectrum of self-assembled TACu(II)Pc film on silver.

Figure 6 shows the active frequency region of the TACu(II)Pc film on silver. Similar spectrum is obtained with Au substrates as well. The Raman bands recorded on the adsorbed films on gold and silver surfaces are compared with the spectra of the thin film of the phthalocyanine on a glass surface as well as phthalocyanine dissolved in dimethylformamide (not shown). Table 1 gives various bands and the corresponding assignments. Raman signals observed for the phthalocyanine macrocycle in the region 600–900  $\text{cm}^{-1}$  are in good agreement with those documented in literature [45–48]. The spectra are dominated by strong in-plane stretching and breathing modes of the macrocycle and are assigned based on the reported literature [45–48]. The stretching vibration involving the bridging nitrogen on the macrocycle is observed at 1395  $\text{cm}^{-1}$ . The macrocyclic vibration observed at 1106  $\text{cm}^{-1}$  may be due to  $-\text{C}=\text{C}-$  and  $-\text{C}-\text{H}$  bonds. Both bands are observed to be very intense. A band corresponding to  $\delta\text{C}-\text{H}$  appears at 1272  $\text{cm}^{-1}$  on both the metal substrates. The relative intensity of the benzene breathing signal observed at  $\sim 954$   $\text{cm}^{-1}$  is higher on Ag than on gold. The pyrrole ring out-of-plane deformation appears at 736  $\text{cm}^{-1}$  and the out-of plane  $\text{C}-\text{H}$  bending vibration appears at 749  $\text{cm}^{-1}$  [47]. The relative intensity of the 736  $\text{cm}^{-1}$  band is higher on silver than on gold. The stretching vibration of the isoindole ring is observed at 1490  $\text{cm}^{-1}$  on the glass surface while it is shifted to 1484  $\text{cm}^{-1}$  on Au and to 1472  $\text{cm}^{-1}$  on Ag.

**Table 1** FT-Raman spectral bands of TACu(II)Pc films on Ag, with the respective assignments; Relative intensities are given in brackets.

Raman shift, $\text{cm}^{-1}$	Assignments
1608(21)	$\delta\text{NH}_2$
1581(28)	Benzene ring stretching
1538(51)	$\gamma\text{C}\alpha\text{N}\alpha$
1487(77)	Iso-indole ring stretching
1395(100)	$\gamma\text{C}\alpha\text{N}\beta$ , $\gamma\text{C}\beta\text{C}\beta$
1355(60)	$\gamma\text{C}\beta\text{C}\beta$ , $\gamma\text{C}\alpha\text{N}\alpha$
1318(57)	Pyrrole stretch
1272(70)	$\gamma\text{CN}(\text{NH}_2)$
1143(66)	$\delta\text{CCC}$ , $\gamma\text{C}\alpha\text{N}\beta$
1106(87)	$\gamma\text{CC}$ , $\delta\text{CH}$
991(06)	$\delta\text{CH}$
948(04)	Benzene breathing
750(57)	$\delta\text{CH}$ , $\delta\text{CCC}$
736(40)	Pyrrole ring out-of-plane bending
659(47)	Macrocycle breathing
597(28)	Benzene ring deformation
572(36)	Out-of-plane ring deformation
236(23)	Ag–N stretching

$\gamma$  Stretching;  $\delta$ , Bending;  $\alpha$  and  $\beta$  are indicated in Fig. 1.

The adsorption process leads to an interaction of the metal with the nitrogen of the amino group, and this would give rise to a metal-nitrogen stretch. Indeed, an intense band is seen in the case of the molecular film on silver surface at 236  $\text{cm}^{-1}$ . This is absent in the case of glass slide as well as the solution spectra. This signal is assigned to Ag–N stretching mode of vibration [49]. The relative intensities corrected for the base line are different on silver as compared to gold surface. This aspect of surface enhanced Raman scattering studies will be reported elsewhere.

## CONCLUSIONS

Tetraamino metal phthalocyanines adsorb onto gold and silver electrodes with the nitrogens anchoring onto the metal surface. The surface coverage is fairly high and close to a monolayer on both metal substrates. Preliminary investigations reveal that the tetraamino cobalt phthalocyanine monolayer film on silver electrodes is very stable and electroactive. The use of these films for the electrocatalytic reduction of oxygen is being explored.

## ACKNOWLEDGMENT

Financial support from the DST and the CSIR, New Delhi, India are gratefully acknowledged.

## REFERENCES

1. C. C. Leznoff and A. B. P. Lever. (Eds.), *Phthalocyanines: Properties and Applications*, VCH, New York, Vol. 1 (1989), Vol. 2 (1993), Vol. 3 (1993), Vol. 4 (1996).
2. N. B. McKewn. *Phthalocyanine Materials*, Cambridge University Press, UK (1998).
3. A. Ulman. *Chem. Rev.* **96**, 1533 (1996).
4. E. Ostuni, L. Yan, G. M. Whitesides. *Colloids Surf. B* **15**, 3 (1999).
5. H. Imahori, H. Norieda, Y. Nishimura, I. Yamazaki, K. Higuchi, N. Kato, T. Motohiro, H. Yamada, K. Tamaki, M. Arimura, Y. Sakata. *J. Phys. Chem. B* **104**, 1253 (2000).
6. L. Yan, W. T. S. Huck, X.-M. Zhao, G. M. Whitesides. *Langmuir* **15**, 1208 (1999).
7. H. Imahori, H. Yamada, Y. Nishimura, I. Yamazaki, Y. Sakata. *J. Phys. Chem. B* **104**, 2099 (2000).
8. S. Semal, C. Bauthier, M. Voue, J. J. V. Eynde, R. Gouttebaron, J. D. Coninc. *J. Phys. Chem. B* **104**, 6225 (2000).
9. S. Jian-Ku, D. Tianbao, J. G. Van Alsten. *Polym. Mater. Sci. Eng.* **81**, 423 (1999).
10. M. J. Cook. *Pure Appl. Chem.* **71**, 2145 (1999).
11. M. J. Cook, R. Hersans, J. McMurdo, D. A. Russell, *J. Mater. Chem.* **6**, 149 (1996).
12. T. R. E. Simpson, D. A. Russell, I. Chambrier, M. J. Cook, A. B. Horn, S. C. Thorpe. *Sens. Actuators B* **29**, 353 (1995).
13. T. R. E. Simpson, D. J. Revell, M. J. Cook, D. A. Russell. *Langmuir* **13**, 460 (1997).
14. D. J. Revell, I. Chambrier, M. J. Cook, D. A. Russell. *J. Mater. Chem.* **10**, 31 (2000).
15. V. Huc, J.-P. Bourgoin, C. Bureau, F. Valin, G. Zalczer, S. Palacin. *J. Phys. Chem. B* **103**, 10489 (1999).
16. Z. Li, M. Lieberman, W. Hill. *Langmuir* **17**, 4887 (2001).
17. L. T. Kubota, Y. Gushikem, J. Perez, A. A. Tanaka. *Langmuir* **11**, 1009 (1995).
18. M. R. Hempstead, A. B. P. Lever, C. C. Leznoff. *Can. J. Chem.* **65**, 2677 (1987).
19. Y.-H. Tse, P. Janda, H. Lam, J. Zhang, W. J. Pietro, A. B. P. Lever. *J. Porphyrins Phthalocyanines* **1**, 3 (1997).
20. B. N. Achar, G. M. Fohlen, J. A. Parker, J. Keshavayya. *Polyhedron* **6**, 1463 (1987).
21. Y.-H. Tse, P. Janda, H. Lam, A. B. P. Lever. *Anal. Chem.* **67**, 981 (1995).
22. M. P. Somashekarappa and J. Keshavayya. *Synth. React. Inorg. Met.-Org. Chem.* **31**, 811 (2001).
23. M. A. Brayant and J. E. Pemberton. *J. Am. Chem. Soc.* **113**, 8284 (1991).
24. P. Cario, J. C. Rubim, R. Aroca. *Langmuir* **14**, 4162 (1998).
25. H. Angerstein-Kozłowska. In *Comprehensive Treatise of Electrochemistry*, Vol. 9, E. Yeager, J. O' M. Bockris, B. E. Conway, S. Sarangapani (Eds.), p. 24, Plenum, New York (1994).
26. P. Waszczuk, P. Zelenay, J. Sobkowski. *Electrochim. Acta* **43**, 1963 (1998).
27. W. Kalz and H. Homborg. *Z. Naturforsch.* **38B**, 470 (1983).
28. M. D. Porter. T. B. Bright. D. L. Allara. C. E. D. Chidsey. *J. Am. Chem. Soc.* **109**, 3559 (1987).

29. C. E. D. Chidsey and D. N. Loiacono. *Langmuir* **6**, 682 (1990).
30. S. E. Creager and K. G. Olsen. *Anal. Chim. Acta* **307**, 277 (1995).
31. C. Amatore, J. M. Saveant, D. Tessier. *J. Electroanal. Chem.* **147**, 39 (1983).
32. J. Zagal, P. Bindra, E. Yeager. *J. Electrochem. Soc.* **127**, 1506 (1980).
33. J. Zagal, M. P'aez, A. A. Tanaka, J. R. Dos Santos, Jr., C. A. Linkous. *J. Electroanal. Chem.* **339**, 13 (1992).
34. J. Ouyang, K. Shigehara, A. Yamada, F. C. Anson. *J. Electroanal. Chem.* **297**, 489 (1991).
35. P. Janda, N. Kobayashi, P. R. Auburn, H. Lam, C. C. Leznoff, A. B. P. Lever. *Can. J. Chem.* **67**, 1109 (1989).
36. N. Kobayashi, P. Janda, A. B. P. Lever. *Inorg. Chem.* **31**, 5172 (1992).
37. A. B. P. Lever, E. R. Milaeva, G. Speier. In *Phthalocyanines: Properties and Applications*, Vol. 3, C. C. Leznoff and A. B. P. Lever (Eds.), pp. 1–69, VCH, New York (1993).
38. E. Laviron. *J. Electroanal. Chem.* **52**, 355 (1974).
39. N. Kobayashi, H. Lam, W. A. Nevin, P. Janda, C. C. Leznoff, A. B. P. Lever. *Inorg. Chem.* **29**, 3415 (1990).
40. A. Bettelheim, B. A. White, S. A. Raybuck, R. W. Murray. *Inorg. Chem.* **26**, 1009 (1987).
41. K. L. Brown and H. A. Mottola. *Langmuir* **14**, 3411 (1998).
42. C. A. Jennings, G. J. Kovacs, R. Aroca. *J. Phys. Chem.* **96**, 1340 (1992).
43. S. Ushioda. *J. Electron. Spectrosc. Relat. Phenom.* **54–55**, 881 (1990).
44. J. Zhao and R. L. McCreery. *Langmuir* **11**, 4036 (1995).
45. O. V. Quinzani, A. H. Jubert, P. J. Aymonino. *J. Raman Spectrosc.* **20**, 141 (1989).
46. A. A. McConnell, J. A. Nimmo, W. E. Smith. *J. Raman Spectrosc.* **20**, 375 (1989).
47. B. Simic-Glavaski, S. Zecevic, E. B. Yeager. *J. Electroanal. Chem.* **150**, 469 (1983).
48. R. Aroca, C. Jennings, R. O. Loutfy, A.-M. Hor. *Spectrochim. Acta A* **43**, 725 (1987).
49. J. A. Creighton, C. G. Blatchford, M. G. Albrecht. *J. Chem. Soc. Faraday Trans. II* **75**, 790 (1979).